Supporting Information

Simultaneously improved photoluminescence, stability, and carrier transport of perovskite nanocrystals by post-synthetic perfluorobutanesulfonic acid treatment

Xiao Huang, Xinli Wang, Jie Gao, Yang Sun, Jun Zhan, Yi Wang,* Xi-Cheng Ai and Jian-Ping Zhang

Key Laboratory of Advanced Light Conversion Materials and Biophotonics, Department of Chemistry, Renmin University of China, Beijing 100872, China

E-mail: ywang@ruc.edu.cn

S1 Experimental section

Materials

Oleic acid (OA, AR, Mreda), Nonafluorobutanesulfonic acid hydrate (PFBA, 98%, Shanghai Meryer), n-Octane (99%, Shanghai Meryer), Lead(II) bromide (PbBr$_2$, 99.99%, Rhawn), Oleylamine (OAm, 90%, Rhawn), 1-Octadecene (ODE, 90%, Heowns), Cesium carbonate (Cs$_2$CO$_3$, 99.99%, 3Achemical), Hexyl hydride (C$_6$H$_{14}$, AR, Tgchem), and Methyl acetate (MeOAc, 98%, Energy-chemical).

Instruments

X-ray diffraction (XRD) spectra were recorded on a Shimadzu XRD-7000 diffractometer using Cu Kα radiation in the 2θ range from 10° to 50° at a scanning rate of 2° per min. Steady-state photoluminescence (PL) spectra, PL quantum yield (PLQY), and time-resolved PL (TRPL) were taken using an Edinburgh FLS 980 spectrometer. Specifically, for the TRPL measurement, the excitation light pulse was provided using a picosecond diode laser at a 405 nm wavelength, and the detection wavelength was 515 nm. In-situ PL spectra were recorded by a fiber optic spectrometer (AvaSpec-ULS2048x64), where the sample was excited by a continuous-wave laser (MTO M-33A450-1W-G, excitation wavelength: 450 nm) whose pump intensity was regulated by a neutral density filter. Transmission Electron Microscope (TEM) images were acquired by a JEOL JEM-2100 microscope operated at 200 kV. Electrochemical impedance spectroscopy (EIS) and space-charge limited current (SCLC) measurements were conducted on an FTO/ZnO/perovskite/Al device. EIS was performed using ZAHNER PP211 with a frequency range from 0.1 to 10^6 Hz, and SCLC was measured by a Keithley 4200 source meter with a voltage range of –0.3 V to 7.0 V in the dark. The X-ray photoelectron spectroscopy (XPS) experiment was conducted using an X-ray photoelectron spectrometer (ThermoFisher, ESCALAB 250Xi, USA). The vacuum level in the analysis chamber was kept at 8×10^{-10} Pa, and the excitation source of Al Kα radiation ($hv = 1486.6\ eV$) was working at an operating voltage of 12.5 kV and a

filament current of 16 mA. The pass energy for the full spectrum testing was set at 100 eV with a narrow spectrum at 30 eV. The step size was 0.05 eV, and the dwell time ranged from 40 to 50 ms. Charge correction was performed using the binding energy of C1s =284.80 eV as the energy standard. All the recorded signals were accumulated over 10 cycles.

Synthesis of Cesium Precursor

0.777 g of Cs_2CO_3, 36 mL of 1-octadecene (ODE), and 4 mL of oleic acid (OA) were added into a 100 mL three-neck flask and dried for 30 minutes at 120 °C. The mixture was then heated to 120 °C under N_2 environments until the total dissolution of the Cs_2CO_3 powders. The as-obtained Cs-oleate solution (*i.e.*, cesium precursor) was stored in a refrigerator at −18 °C for future use.

Synthesis of CsPbBr$_3$ QDs

0.134 g of $PbBr_2$, 10 mL of 1-octadecene (ODE), 2 mL of oleic acid (OA), and 2 mL of oleylamine (OAm) were added into a 100 mL flask. The mixture was first dried at 80 °C for 1 hour under vacuum, and then the temperature was raised to 185 °C under N_2 flow. Subsequently, 0.7 mL of the cesium precursor solution as has been preheated at 100 °C was swiftly injected into the flask. After a 30-second reaction, the reaction is swiftly quenched by immersing the flask in an ice bath. The as-obtained colloidal solution was sealed and stored in a refrigerator at −18 °C for future use.

CsPbBr$_3$ QDs Purification, Ligand Exchange, Preprocessing for Film Fabrication

(1) **Purification (washing):** 3 mL of methyl acetate was added to 1 mL of CsPbBr$_3$ QDs solution followed by centrifugation at 12,000 rpm for 5 minutes. After discarding the supernatant, the precipitates were dispersed in 1 mL of *n*-hexane.

(2) **Ligand exchange:** 1 mL of the purified solution was transferred to a tube for ligand exchange. For the untreated and PFBA-treated samples, the purified solution was mixed with 0.2 mL of the OA/OAm solution (*i.e.*, 250 µL of OA

and 250 μL of OAm dissolved in 10 mL of *n*-hexane) and 0.2 mL of the PFBA-OAm solution (*i.e.*, 100 μL PFBA and 250 μL OAm mixed in 10 mL of *n*-hexane), respectively, under vigorous stirring for 20 minutes. Then, 1.2 mL of methyl acetate was added to the solution, and the mixture was centrifuged at 12,000 rpm for 5 minutes. The supernatant was discarded, while the precipitates were dispersed in *n*-hexane to obtain the colloidal solution with a concentration of 20 mg/mL. In quantitative, by calculating the integrated area of the characteristic peaks of C and F from the XPS data, the molar ratio of the PFAM to OA/OAm is estimated to be ~1:4.

(3) ***Preprocessing for film fabrication***: an equal volume of methyl acetate was added to the aforementioned untreated and PFBA-treated QDs solutions, and the mixed solution was centrifuged at 12,000 rpm for 5 minutes. The precipitates were separated and dispersed in 0.5 mL of octane, which was further used for QD film fabrication.

Preparation of the CsPbBr₃ QDs-based devices

(1) FTO/ZnO/QD/Al device fabrication. Fluorine-doped tin oxide (FTO) glass was first washed with deionized water containing detergent, acetone, and ethanol subsequently. After being dried with the N_2 flow, the FTO glass was processed with a 15-minute UV-ozone treatment. Next, a solution of zinc oxide nanoparticles in ethanol (50 mg/mL) was spin-coated onto the FTO substrate at 4000 rpm for 30 seconds. Following the thermal annealing at 100 °C for 30 minutes to remove excess solvent and solidify the zinc oxide layer, ~50 μL of the QDs solution was spin-coated at 2000 rpm for 30 seconds. At last, a 100 nm-thick layer of aluminum was deposited using a high-vacuum thermal evaporation system to form the metal electrode.

(2) ITO/NiO_x/QD/Au device fabrication. Indium-doped tine oxide glass was first washed with deionized water containing detergent, acetone, and ethanol subsequently. After being dried with the N_2 flow, the ITO glass was processed with a 15-minute UV-ozone treatment. Then a solution of nickel oxide nanoparticles in water (30 mg/mL) was spin-coated onto the ITO at 3000 rpm for 30 seconds followed by the thermal

annealing at 150 °C for 30 minutes. At last, ~50 μL of the QDs solution was spin-coated at 2000 rpm for 30 seconds, and an 80 nm-thick layer of gold was deposited using a high-vacuum thermal evaporation system to form the metal electrode.
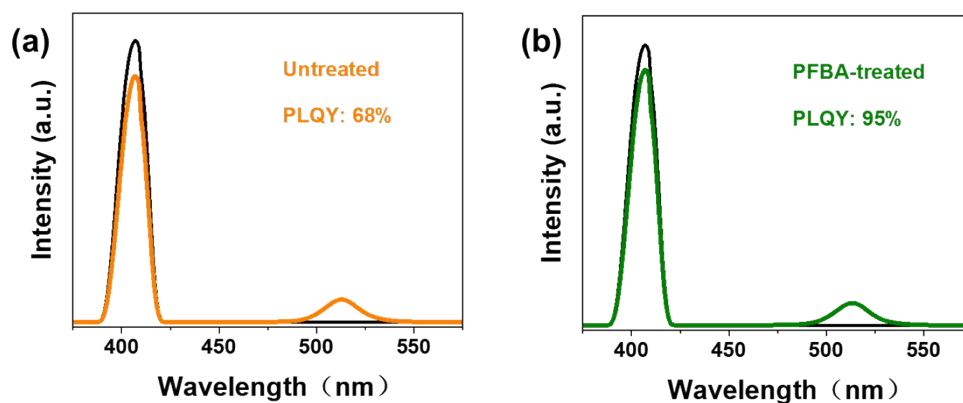
S2. PLQY of CsPbBr₃ perovskite QDs solutions

Fig. S1. PLQY of CsPbBr₃ perovskite QDs solutions without (a) and with (b) the PFBA post-treatment.

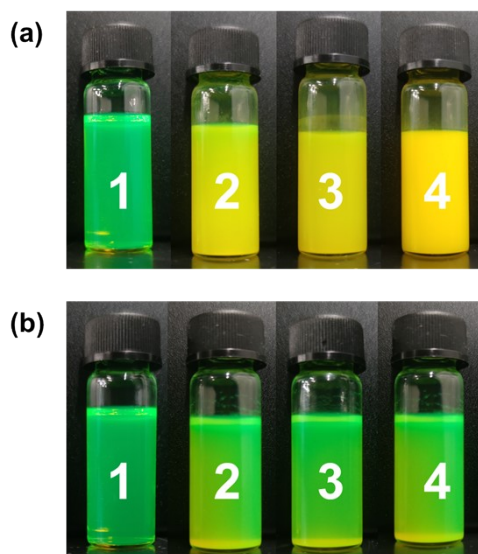## S3. Photographs of CsPbBr₃ QDs solutions with different washing times

Fig. S2. Photographs of CsPbBr$_3$ QDs solutions without (a) and with (b) the PFBA post-treatment under room light as a function of purification times.
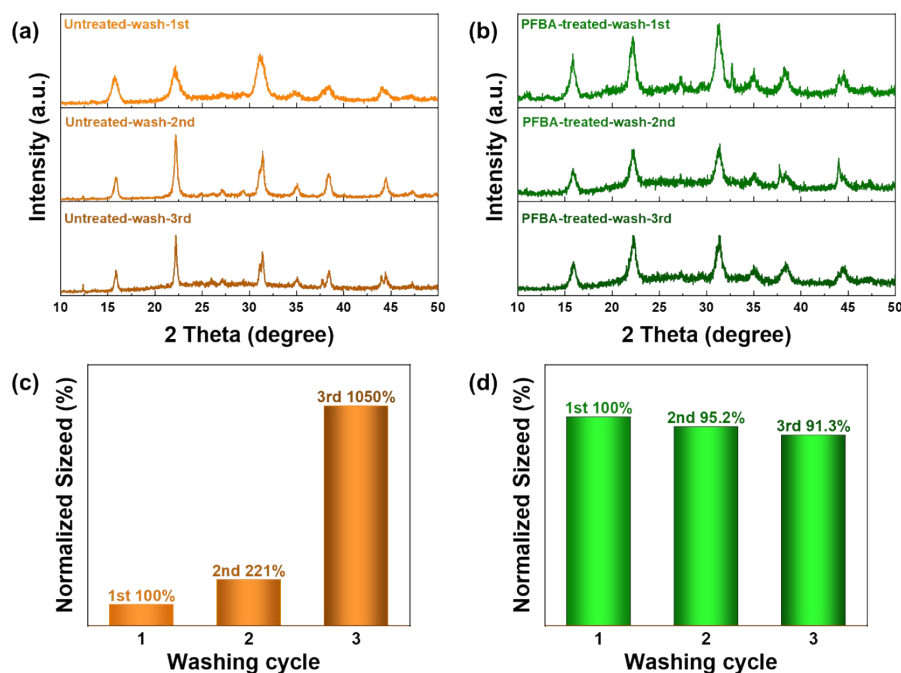
S4. X-ray diffraction (XRD) characterization

Fig. S3. XRD patterns of CsPbBr$_3$ QDs solutions without (a) and with (b) the PFBA post-treatment as a function of purification times. (c, d) The relative value of the calculated grain size, where the orange and green bars denote the untreated and PFBA-treated samples, respectively.

The crystalline sizes of perovskite films can be calculated from the width of XRD peaks by using Debye Scherrer equation,[1]

$$D = \frac{K\lambda}{\beta cos\theta}$$

where D is the average grain size, K is the Scherrer constant, typically between 1 and 1.2 depending on experimental conditions and the nature of the crystal, λ is the wavelength of the incident X-rays, β is the full-width-half-maximum (FWHM) of the targeted X-ray diffraction peak, and θ is the diffraction angle.

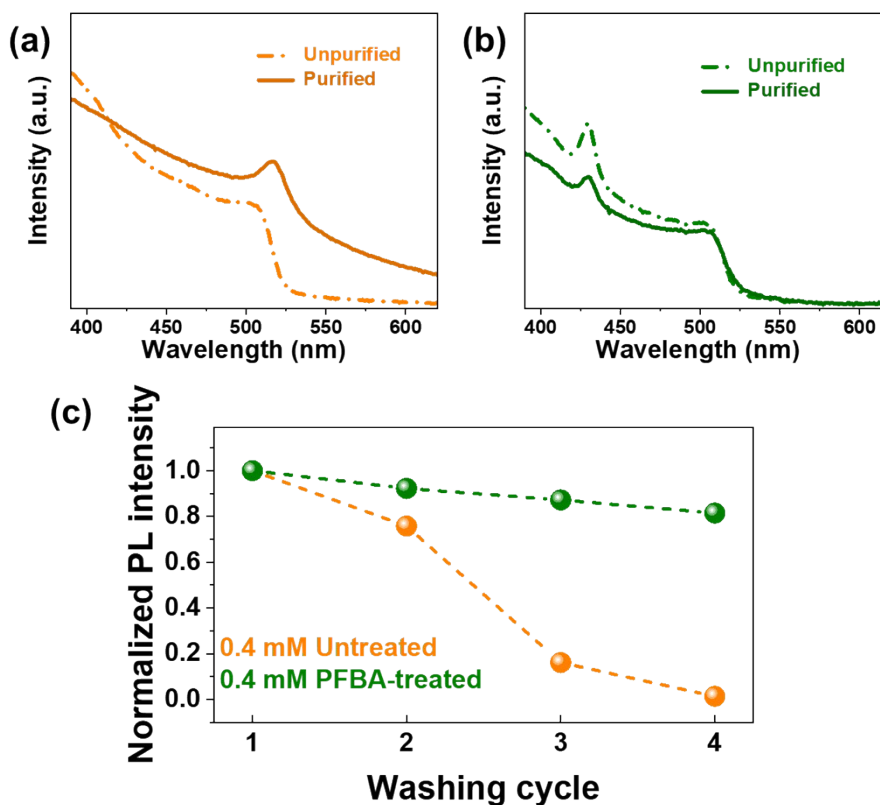## *S5. Quantum dots with different washing times*

Fig. S4. (a, b) Steady-state UV-vis absorption of $CsPbBr_3$ perovskite QDs solutions before and after purification, where the orange and green curves denote untreated and PFBA-treated samples. The subgap signals above 530 nm arise from the Rayleigh scattering of the nanocrystals. (c) PL intensity evolution of $CsPbBr_3$ QDs solutions as a function of washing cycles.

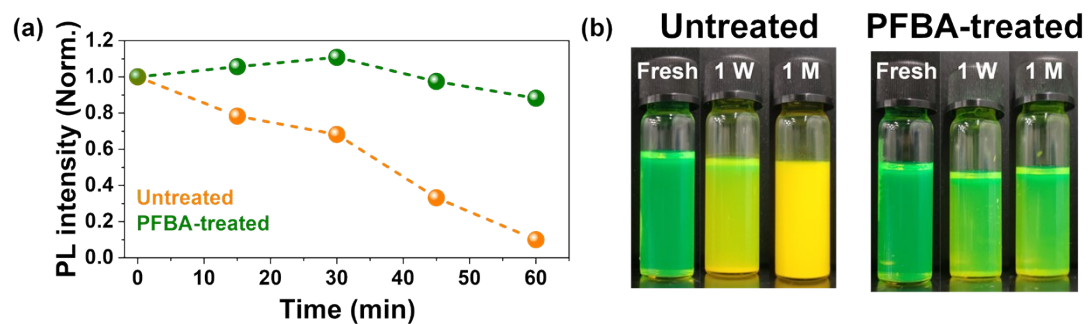## S6. Thermal stability and storage stability of quantum dots

Fig. S5. (a) PL intensity evolution of $CsPbBr_3$ QDs films as a function of thermal annealing time. (b) Photographs of $CsPbBr_3$ QDs solutions stored in the ambient environment for different times.

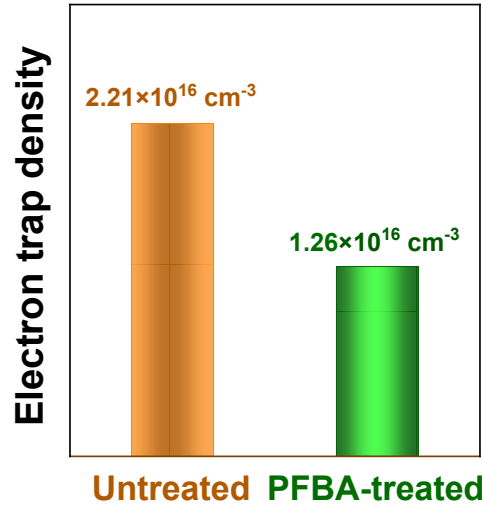## S7. Electron trap density calculation based on SCLC data

Fig. S6. Electron trap densities of the CsPbBr$_3$ QD films without and with the PFBA treatment as derived from the SCLC data (see details in the text below).

The characteristic $I - V$ response measured by SCLC is fitted to the power-law function ($I \propto V^n$) to evaluate the trap-filling process. In brief, with the increase of bias voltage, trap states are gradually filled. The saturation of trap states with charge carriers is mirrored by a trap-filled limit voltage (V_{TFL}), above which the power index sharply increases. Thus, the trap density (n_{trap}) can be calculated from:[2]

$$n_{trap} = \frac{2\varepsilon_0 \varepsilon V_{TFL}}{eL^2}$$

where ε is the relative dielectric constants of CsPbBr$_3$ ($\approx$22),[3] ε_0 is the vacuum permittivity, and L is the thickness of QD films. The n_{trap} values are calculated to be 2.21×10^{16} cm^{-3} and 1.26×10^{16} cm^{-3} for the untreated and PFBA-treated films respectively.

S8. Space charge limited current (SCLC) from hole transporting layer-only devices
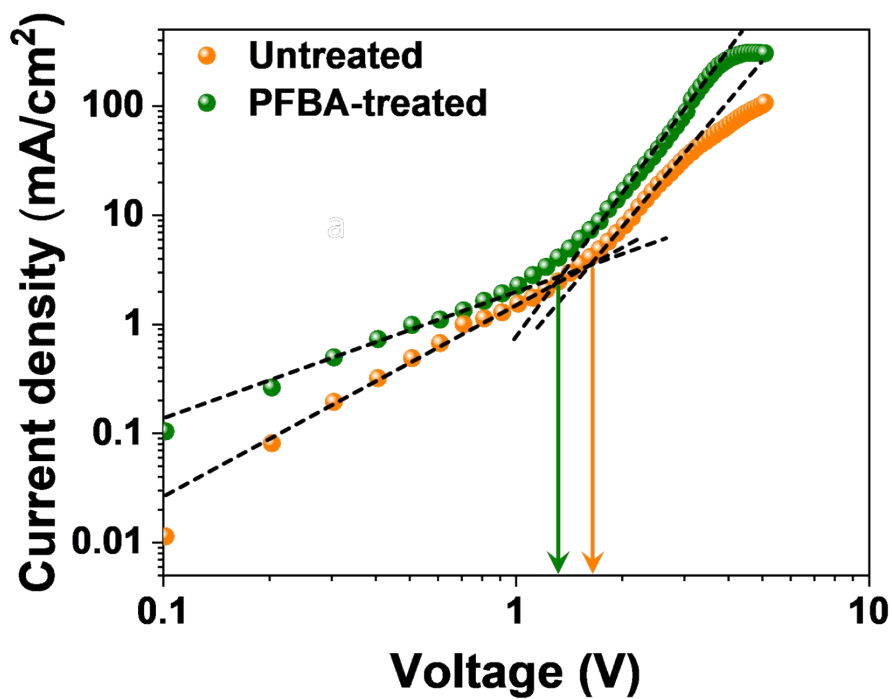

Fig. S7. Dark current-voltage responses of the hole transporting layer-only devices without (orange) and with (green) the PFBA post-treatment, respectively.

S9. Electrochemical impedance spectroscopy (EIS) characterization
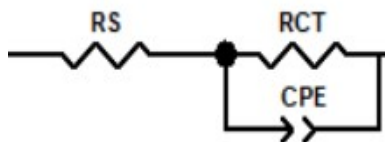
.

Fig. S8. The equivalent circuit model used for electrochemical impedance spectroscopy analysis.

The equivalent circuit model invoked to analyze the EIS results is shown in Figure S8, where R_S, R_{CT}, and CPE represent the charge transfer resistance, charge transfer resistance, and chemical capacitance, respectively. Based on the first and second x-intercept of the Nyquist plot (Figure 3d), R_S and R_{CT} values can be obtained. On the other hand, the CPE value is derived from the circuit fitting results and regarded as a constant phase element.

References:

1. Y. Ji, M. Wang, Z. Yang, H. Wang, M. A. Padhiar, J. Shi, H. Qiu and A. S. Bhatti, *J. Phys. Chem. C*, 2022, **126**, 1542-1551.
2. A. Ng, Z. Ren, H. Hu, P. W. Fong, Q. Shen, S. H. Cheung, P. Qin, J. W. Lee, A. B. Djurišić and S. K. So, *Adv. Mater.*, 2018, **30**, 1870329.
3. M. I. Saidaminov, M. A. Haque, J. Almutlaq, S. Sarmah, X. H. Miao, R. Begum, A. A. Zhumekenov, I. Dursun, N. Cho and B. Murali, *Adv. Optical Mater.*, 2017, **5**, 1600704.